C. Prablanc, D. Pélisson and Y. Rossetti (Eds.)
Progress in Brain Research, Vol. 142

CHAPTER 11

Internal forward models in the cerebellum: fMRI study on grip force and load force coupling

Mitsuo Kawato [1,*], Tomoe Kuroda [2], Hiroshi Imamizu [1], Eri Nakano [1], Satoru Miyauchi [3] and Toshinori Yoshioka [1]

[1] *ATR Human Information Science Laboratories, 2-2-2, Hikaridai, Seika-cho, Soraku-gun, Kyoto 619-0288, Japan*
[2] *JST/ERATO Kawato Dynamic Brain Project, 2-2-2, Hikaridai, Seika-cho, Soraku-gun, Kyoto 619-0288, Japan*
[3] *Communications Research Laboratory, 588-2, Iwaoka, Iwaoka-cho, Nishi-ku, Kobe, Hyogo 651-2492, Japan*

Abstract: Internal models are neural mechanisms that can mimic the input–output or output–input properties of the motor apparatus and external objects. Forward internal models predict sensory consequences from efference copies of motor commands. There is growing acceptance of the idea that forward models are important in sensorimotor integration as well as in higher cognitive function, but their anatomical loci and neural mechanisms are still largely unknown. Some of the most convincing evidence that the central nervous system (CNS) makes use of forward models in sensory motor control comes from studies on grip force–load force coupling. We first present a brief review of recent computational and behavioral studies that provide decisive evidence for the utilization of forward models in grip force–load force coupling tasks. Then, we used functional magnetic resonance imaging (fMRI) to measure the brain activity related to this coupling and demonstrate that the cerebellum is the most likely site for forward models to be stored.

Introduction

Internal models are neural mechanisms located inside the brain that can mimic the input–output properties of the motor apparatus and external objects (located outside the brain), or their inverse transformations. Forward internal models predict sensory consequences of executed movements from information on efference copies of motor commands, whereas inverse internal models determine the appropriate motor commands from information on the desired motor consequences. Several computational theories have proposed that forward and/or inverse models are learned in the cerebellum (Kawato et al., 1987; Kawato and Gomi, 1992; Miall et al., 1993; Wolpert et al., 1998; Kawato, 1999).

We have accumulated quite convincing data from both electrophysiological studies (Shidara et al., 1993; Gomi et al., 1998; Kitazawa et al., 1998; Kobayashi et al., 1998; Takemura et al., 2001; Yamamoto et al., 2002) and human imaging studies (Imamizu et al., 2000) demonstrating that inverse models are acquired through motor learning based on Purkinje cell synaptic plasticity and stored in the cerebellum. Even though many behavioral (Miall et al., 1993; Wolpert et al., 1995; Flanagan and Wing, 1997; Scarchilli and Vercher, 1999; Mehta and Schaal, 2002) and theoretical studies (Kawato et al., 1987; Jordan and Rumelhert, 1992; Miall et

* Correspondence to: Mitsuo Kawato, ATR Human Information Science Laboratories, 2-2-2, Hikaridai, Seika-cho, Soraku-gun, Kyoto 619-0288, Japan. Tel.: +81-774-95-1058; Fax: +81-774-95-2647;
E-mail: kawato@atr.co.jp

al., 1993; Wolpert and Kawato, 1998; Kawato, 1999) have suggested that forward models are functionally and computationally critical for a broad repertoire of behaviors ranging from sensorimotor integration to higher cognitive function, the anatomical loci and neural mechanisms of forward models are still largely unknown. In addition to their use in sensory–motor control, Blakemore et al. (1998, 1999, 2001)) demonstrated that forward models are used for cancellation of sensory inputs generated by one's own movements; in this series of elegant perceptual studies, they suggested that the forward models are located in the cerebellum (see also Vercher et al., 2003, this volume).

Some of the most convincing evidence showing that the CNS makes use of forward models in sensory–motor control comes from studies on grip force–load force coupling. Grip force–load force coupling is a common phenomenon that has been observed in the following situation. When an object is held in a precision grip (e.g. a grasp between the tips of the thumb and forefinger) and moved by voluntary movements (e.g. arm movements), the grip force perpendicular to the contact surfaces changes in phase with, and in a similar temporal waveform to, the load force induced by the movements (Johansson and Westling, 1984; Flanagan and Tresilian, 1994; Johansson, 1996). The coupling between the two forces prevents the object from slipping while using the minimal grip force. This grip force modulation is anticipatory in the sense that changes in the grip force occur at the same time as, or even prior to, changes in the load force.

Previously we proposed computational models that explain grip force–load force coupling with forward models (Kawato, 1999), and their predictions have been confirmed by recent behavioral studies (Flanagan and Wing, 1996; Vetter et al., 2002). Here, we summarize these previous computational and behavioral studies that demonstrate the utilization of forward models in grip force–load force coupling. Then, we present a functional magnetic resonance imaging (fMRI) experiment that investigates the possible brain loci of the forward models used for the coupling and suggest that the cerebellum is the likeliest site.

Computational models and behavioral experiments that support the use of forward models in grip force–load force coupling

We first briefly explain a simple example of grip force–load force coupling to facilitate clear understanding of the phenomenon. In preparation for the fMRI experiment, we measured grip force and load force outside the MRI scanner to confirm that the two forces were coupled in the current task paradigm (Fig. 1). A subject lay down in a supine position and made cyclic up-and-down arm movements paced by beep sounds (2 Hz) while holding a ping-pong ball between the tips of the thumb and forefinger. At each beep, the subject made a set of up and down strokes above the abdomen. The LED marker of a position recording system (OPTOTRAK, Northern Digital, Inc., Canada) was mounted on top of the object. The marker's vertical position was sampled at 500 Hz. We obtained the object's acceleration due to arm movement by twice differentiating the time series of the position data. Load force was then calculated as the absolute value of the product of the object's acceleration and mass (0.015 kg), where acceleration was the sum of the acceleration due to movement and gravitational acceleration. Grip force was measured by small and light pressure gauges (PS-10KA, Kyowa Electronic Instruments Co., Japan) attached to the contact surfaces. The amplitude of the arm movements was 30–40 cm. Because grip force is coupled with the absolute value of load force, it had two peaks coinciding with the acceleration and deceleration peaks of the arm movement within one cycle. Thus with a 2 Hz movement, the primary frequency of the grip force (solid line in Fig. 1B) and load force modulation was 4 Hz (dotted line in Fig. 1B). As has been reported in numerous studies (Johansson and Westling, 1984; Flanagan and Tresilian, 1994; Johansson, 1996), the grip force was temporally coupled with the load force during movement, and a cross-correlation analysis indicated that the phase of the grip force preceded that of the load force by approximately 15 ms with a correlation coefficient of 0.88. These values are in close agreement with previously reported values for cyclic movement (Flanagan and Wing, 1995).

Previous studies on grip force–load force coupling have suggested that both feedback (Johansson

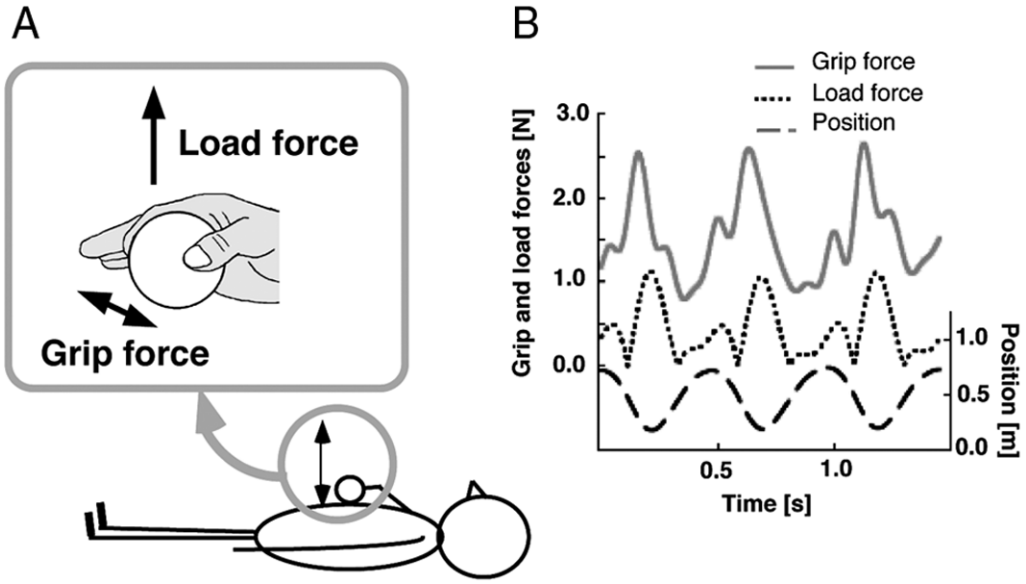

Fig. 1. (A) Experimental setup of grip force–load force coupling in our fMRI study. A subject lay down in a supine position and made cyclic up-and-down arm movements above the abdomen while holding a ping-pong ball between the tips of the thumb and forefinger. (B) A subject's sample record of the temporal pattern of grip force (solid line), load force (dotted line) and vertical position (broken line) of the grasped object. Grip force and load force coupling were observed while transporting a ping-pong ball.

and Westling, 1984) and feedforward (Flanagan and Tresilian, 1994) components are necessary for controlling grip force. Feedback control is important for establishing a stable grip force/load force ratio and for responding to unexpected disturbances, while feedforward control is important for rapid, predictive and accurate coupling of grip force to load force during movement. The fact that the change in grip force precedes the change in load force suggests that pure sensory feedback, which has large (70 ms) time delays, cannot be the sole source of grip force modulation. Therefore the CNS predicts changes in load force to modulate grip force.

There may be a number of computational and neural models that can explain the observed grip force–load force coupling. However, because of the above mentioned predictive nature of grip force modulation, we can assume that either forward or inverse models, or a combination of the two, are utilized in grip–load coupling. Accordingly, there are three models that can potentially explain the observed grip force–load force coupling (Fig. 2). The first model (Fig. 2A) consists of a single inverse dynamics model (IDM) of the combined arm, hand and object dynamics. The combined IDM generates the arm motor command as well as the hand motor command. For generation of hand motor commands, this model is not computationally attractive since the entire IDM must be relearned every time a different hand grasping posture is taken and a different object is manipulated. In other words, this model has the least structural and functional modularity with respect to separation of object manipulation, hand posture control and arm movement control. This model is the least economically compatible in terms of the number of modules required when it is combined with the MOSAIC structure, that contains multiple models (Wolpert and Kawato, 1998). The second model shown in Fig. 2B has modularity between arm and hand control. The IDM of the arm and object generates the motor command for the arm while receiving the desired trajectory information. The object's IDM predicts the load force necessary to transport the object along the desired trajectory. This load force information is fed to the grip force controller, which generates the hand motor commands required for the grip force that is proportional to the predicted load force. Specifically, the future load force is computed by the object's IDM, which is divided by a friction coefficient and multiplied by

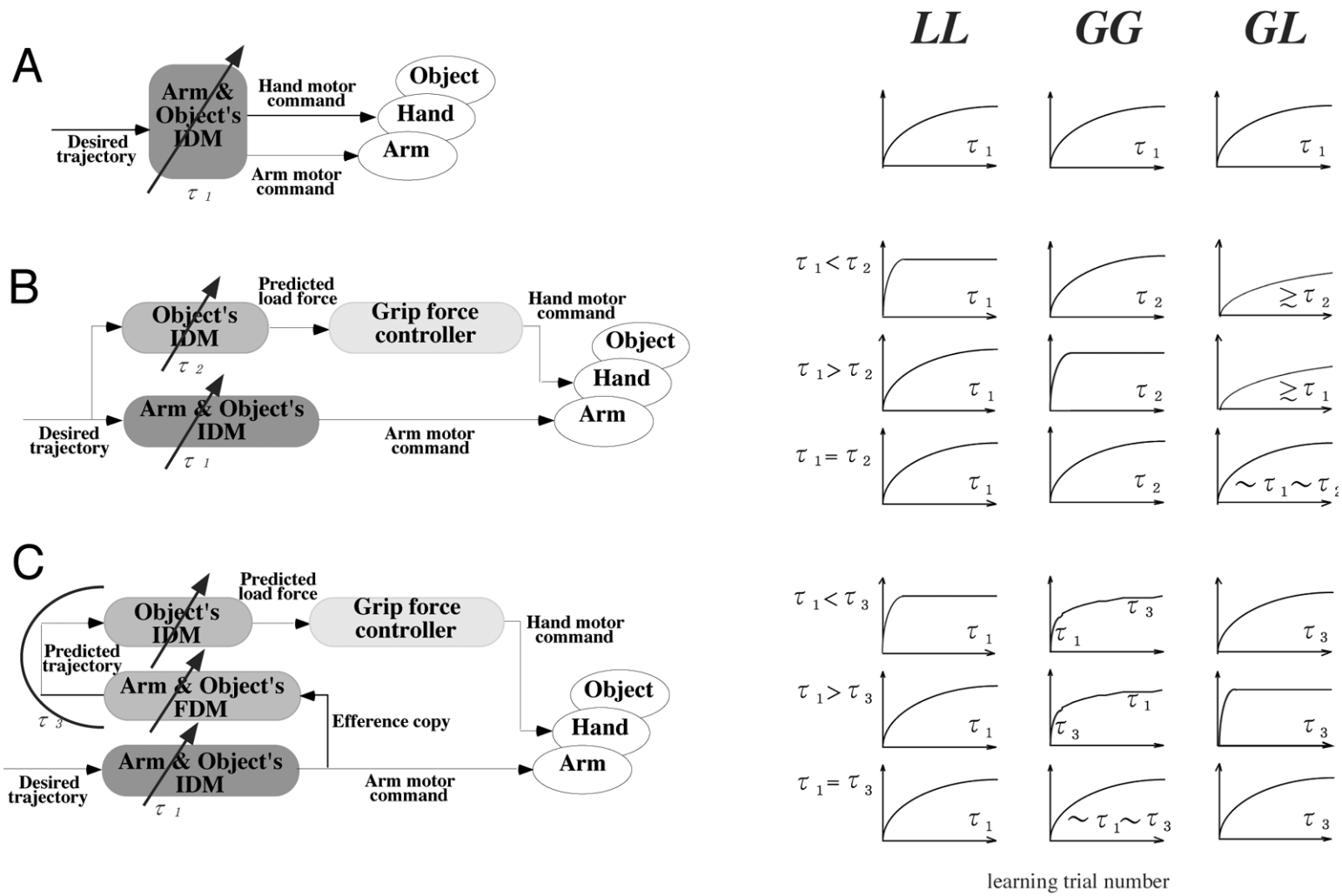

Fig. 2. Three different computational models, A, B, and C, of grip force–load force coupling (left) and their predictions on the auto-correlation and cross-correlation of load (L) and grip (G) forces (right). Only the third model shown in C utilizes the forward model.

CICERO/GALAYAA B.V./Prablanc 11: pp. 171-188

a safety factor to derive an appropriate future grip force. Finally, this necessary force is realized in a predictive manner by the grip force controller.

Kawato (1999) proposed the computational model of grip force–load force coupling shown in Fig. 2C. In this framework, the IDM of the combined dynamics of the arm, hand, and object calculates the appropriate arm motor commands from the desired trajectory of the arm. This command is sent to the arm muscles as well as to the forward model of the combined dynamics of the arm, hand, and object as an efference copy (see also Flanagan and Wing, 1997). The forward model predicts the arm trajectory 50 to 100 ms in the future. From this predicted arm trajectory, a hand motor command is generated in the same way as for the model shown in B. The third model has the largest modularity and utilizes both forward and inverse models of the arm and object. Its extension to multiple models in the framework of MOSAIC (Wolpert and Kawato, 1998) was also proposed by Kawato (1999) so that multiple-object manipulation could be easily switched. Even in the models of B and C, the IDM of the combined arm and object should be relearned or switched every time when a new object is grasped. However, this combined IDM is used for only arm control in B and C, and arm motor commands are less influenced by different object characteristics than hand motor commands, while hand motor command should be drastically altered for different objects. The MOSAIC architecture is best suited for the computational model C, because both the forward and inverse models are utilized, and the learning of object IDM for hand motor command generation is decoupled from learning of arm dynamics.

From the viewpoint of grasp control, the essential difference between models B and C is that the former uses the desired arm trajectory in computing the necessary grip force while the latter uses the arm trajectory estimated by the forward model. If the environment is a well-learned one, the desired arm trajectory is accurately realized and should be similar to the estimated trajectory. Therefore, the behaviors of the two kinds of models are similar and cannot be discriminated between. However, for novel environments that are not well controlled, the desired trajectory and the predicted trajectory could be very different, allowing us to discriminate between the three models. In particular, if one assumes that the forward model is learned more rapidly than the inverse model, an idea consistent with the MOSAIC model, then one would expect good coupling between grip force and load force before good control over the movement trajectory is established.

The right side of Fig. 2 shows predictions of the three models in terms of how three different correlations — involving grip and load forces — will change when learning to manipulate an object with novel dynamics. These correlations are the correlation between load force in a given trial with load force after adaptation (LL), the correlation between grip force in a given trial and grip force after adaptation (GG), and the correlation between the grip force and load force in a given trial. By definition, both LL and GG start from a low value and increase to 1 as learning progresses. From previous studies on grip force–load force coupling, we know that GL takes a high value in the late stages of learning when subjects are well experienced at manipulating the objects (Flanagan and Wing, 1997).

For the single IDM of model A, LL, GG and GL, as shown in the right side of Fig. 2A, should all have a similar rate of increase because a single common neural network generates both hand and arm motor commands as a single unit. If the load dynamics are highly altered, compared with objects subjects are familiar with, the novel dynamics alter the realized trajectory, and induce different acceleration patterns, thus altering the load-force time course while the grip-force time course is inappropriate for the new object and starts from the old pattern for a familiar object. Therefore, at the early stage of learning, GL is low, but as learning progresses both the arm and hand motor commands become appropriate for the new object dynamics, and GL approaches a high value.

Quantitative details of predictions made by model B depend on the relative lengths of the learning time constants of the combined object and arm IDM and the object IDM. The LL-increase time course is determined solely by the learning rate of the combined IDM of arm and object (τ_1), while the GG-increase time course is determined solely by the learning rate of the object IDM (τ_2). At the early phase of learning, after a new object dynamic is imposed, GL is low because the load-force time course is altered,

as in A. As learning progresses, both the combined IDM and object IDM become better models of the controlled objects, and GL increases for two reasons. First, due to combined IDM learning, the desired arm trajectory is better realized and the load force approaches that predicted from the desired trajectory. Secondly, the predicted grip force becomes closer to that required with the new dynamics for the actual arm trajectory because the object IDM improves, and the final realized trajectory approaches the desired trajectory. Consequently, the time course of GL-increase is governed by both of the two time constants of the two IDM learning rates (τ_1 and τ_2). This can also be seen from the block diagram of model B, since GL is the correlation computed through the cascade of the two IDMs (Fig. 2B).

For the third model, C, GL is determined by the third time constant (τ_3) of the forward model of the arm and object as well as the object IDM because the predicted arm trajectory can be close to the actual trajectory even if it is greatly distorted only if the forward model is good. On the other hand, GG is governed by both the third time constant (τ_3) and the first time constant (τ_1), because the grip-force time course is determined by the cascade of all four elements in C (combined IDM and FDM, object IDM, and grip controller). Quantitative details of the time courses of LL, GG and GL differ depending on relative lengths of the learning time constants of each of the different elements within these models. However, regardless of this we can make some qualitative predictions. For the model A, the GL rise rate is exactly the same as those of GG and LL. For the model B, the GL rise rate is not larger than that of either LL or GG. Only model C can have a GL rise rate higher than that of LL. This will occur if the learning rate of the combined IDM (τ_1) is slower than that of the forward model (τ_3). As described below, recent experimental data unequivocally support model C's predictions, and the utilization of forward models is strongly supported.

Behavioral studies done by Flanagan and Wing (1996, 1997) supported model C. In their experiments, they changed the dynamics of manipulated objects by using a one-degree-of-freedom robotic manipulator. This alternation of the object's dynamics significantly disrupted both the hand trajectory and the grip force–load force coupling. Even in these novel situations generated by inertia, viscous, or spring force, grip and load forces became closely coupled after a relatively small number of learning trials, whereas the learning of the hand trajectory was much slower. In other words, during early learning trials, good grip force–load force coupling was quickly acquired even though the arm velocity profile was irregular and poorly controlled. One of the limitations of these studies is that grip–load correlations were examined across learning trials where the load force waveform was changing. Recently, Vetter et al. (2002) dealt with this potential confound by having subjects produce trajectories — after having adapted to the novel load — that were similar to those observed in early learning. They found that after some four learning trials, subjects generated grip–load coupling that was similar to that observed after adaptation and for similar movements (and hence load force waveforms). Consequently, utilization of forward models in grip force–load force coupling is well established. Based on this, we have explored the possible sites of forward models through fMRI experiments.

Materials and methods

Subjects

Three females (ranging in age from 25 to 31) and three males (from 27 to 43) participated in the experiment after giving written informed consent. The protocol was approved by the ethics committee of CRL. All subjects were right-handed.

Task and procedure

The transporting task shown in Fig. 1A includes three components: arm movement control, grip force modulation, and coordination of arm movement and grip force. Therefore, if we remove the first two components, we can extract the brain activity exclusively related to coordination or, more specifically, to forward models. We used a 2 by 2 factorial design of tasks to compare neural activity under conditions with and without arm movement and with and without grip force modulation (Fig. 3). Accordingly, the experimental tasks were (A) transporting an object, (B) loaded arm movement, (C) grip force modula-

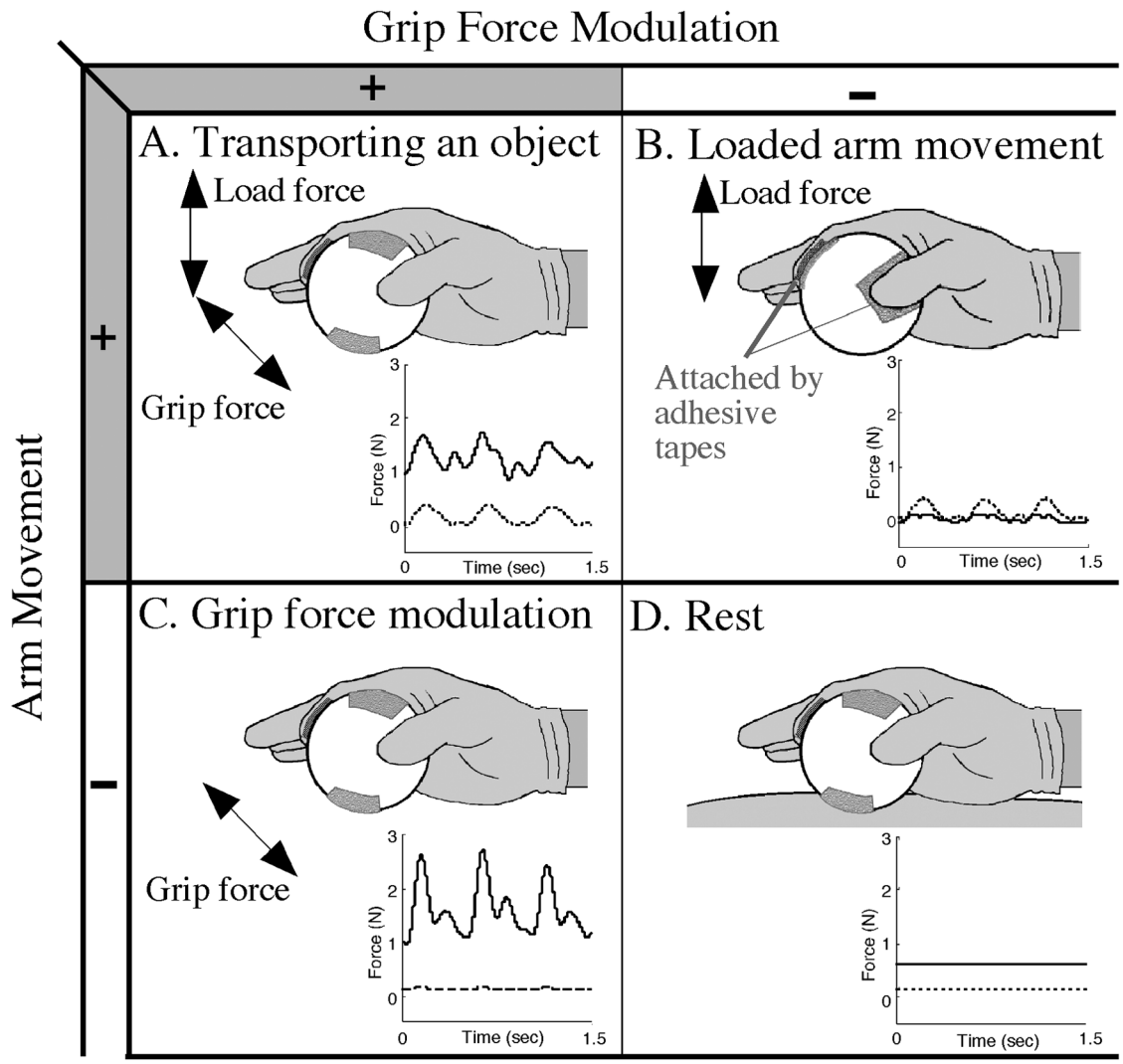

Fig. 3. A 2 × 2 factorial design (with/without arm movement/grip force modulation) of four tasks in the fMRI experiment. The solid lines in the inset boxes depict temporal patterns of grip force, and the dotted lines depict temporal patterns of load force. These measurements were made during behavioral experiments performed outside of the MRI scanner under similar experimental conditions (see section 'Materials and methods').

tion, and (D) rest. In all four tasks, the subjects wore a glove. In the transport and loaded arm movement tasks, movement amplitude was 20–25 cm because of the limited workspace in the gantry. The glove did not alter the basic coupling between grip force and load force (compare Fig. 1 and the inset of Fig. 3A). The loaded arm movement task was similar to the transport task except that the object was attached at the tips of the thumb and forefinger by removable adhesive tape. In this case, grip force modulation is not necessary, and the actual grip force modulation was very small as shown by the solid line in the inset of Fig. 3B. In retrospective inquiries, subjects reported that they were not conscious about the absence of grip force modulation in the loaded arm movement task. Thus, it is unlikely that some kinds of voluntary suppression of grip force in the loaded arm movement condition took place, and this factor influenced brain imaging data. The pressure gauges were attached to the glove underneath the adhesive

tape rather than on the ping-pong ball to avoid any artifact caused by the adhesive tape. During the grip force modulation condition, the subjects held the object in the same grip as in the transport task and periodically changed the grip force voluntarily at 4 Hz (see the inset of Fig. 3C). They were instructed to produce a larger grip force than in the transport task. In the rest period, they made no overt movements. For brevity, the three task conditions A, B and C will be called transport, arm and grasp movements, respectively.

The dynamics of both arm movement and hand configuration were similar in the two arm-movement tasks (A and B) because the object was attached to the fingers during loaded arm movement. Thus, arm motor commands, hand motor commands for hand and finger postural maintenance, and the proprioceptive feedback would also be expected to be similar in these two tasks. Furthermore, the preliminary measurement outside the scanner confirmed that grip force changes that occurred during the grip force modulation task were as large as, or larger than, changes during the transport task (compare the insets of Fig. 3A and 3C). Consequently, finger tactile feedbacks due to modulation of grip forces perpendicular to contact surfaces would be expected to be similar in these two tasks (A and C). Because volitional control of grip force in the grip force modulation task (C) may be more demanding than automatic adjustment of the force in the transport task (A), the subtraction of the signal values in the grasping task from those in the transport task could cause an underestimation of the brain activity related to components other than the grasping component in the transport. However, more importantly it is unlikely that such activation was overestimated.

Each subject performed the tasks with her or his dominant, right arm and hand. Their heads were fixed by using individually molded bite bars. An experimental session consisted of four blocks; in each block, and for all subjects, each of the four task periods occurred for 35.2 s in the fixed order of A, B, C and D as shown in Fig. 3. The subjects prepared for the task during the first 4.4 s of each task period, and performed the task for the successive 30.8 s. Eight functional image volumes of the whole brain were acquired in each task period. Thus, total 128 volumes were acquired in each session.

Brain imaging

A 1.5 T Magnetom Vision system (Siemens, Erlangen) was used to acquire both sixteen axial gradient-echo, echo-planar $T2^*$ weighted image volumes [TR = 4.4 s, TE = 66 ms, flip angle = 90°, thickness = 7 mm, slice gap = 2.8 mm, in-plane resolution = 2 mm × 2 mm] and T1 weighted structural image volumes for anatomical co-registration [TR = 560 ms, TE = 6 ms, flip angle = 90°, thickness = 7 mm, slice gap = 2.8 mm, in-plane resolution = 1 mm × 1 mm]. Each session began with two 'dummy' scans, the data of which were discarded to allow for T1 equilibration effects. Each subject participated in six separate sessions of functional imaging. All the multiple session data were analyzed at once in the following two methods. Session-specific effects were modeled and removed as confounding effects in the general linear model explained below.

Analyses

We used SPM99 [http://www.fil.ion.ucl.ac.uk/spm] for all of the preprocessing and statistical inference procedures except motion correction. To remove motion artifacts, all volumes of each functional imaging session were realigned to the reference, the 65th volume, by using AIR3.08 [http://bishopw.loni.ucla.edu/AIR3]. After that, they were stereotactically normalized using affine and nonlinear transformation and then resampled using sinc interpolation into the space of a standard brain. The volumes were then smoothed with a Gaussian kernel of 4 mm full-width half-maximum (FWHM). The first two image volumes of each task period were regarded as a preparation phase and discarded in order to avoid the effects of task transition, and six other volumes were regarded as a test phase. High-frequency noises were removed with a Gaussian filter (FWHM = 4 s).

?#1

Condition and session effects were estimated according to the general linear model at each and every voxel with delayed boxcar waveforms. To investigate regionally specific condition effects of interest, the estimated coefficients were compared using appropriately weighted linear contrasts (Friston et al., 1995). In the first half of the analyses to obtain transport > rest, grasp > rest, and arm > rest con-

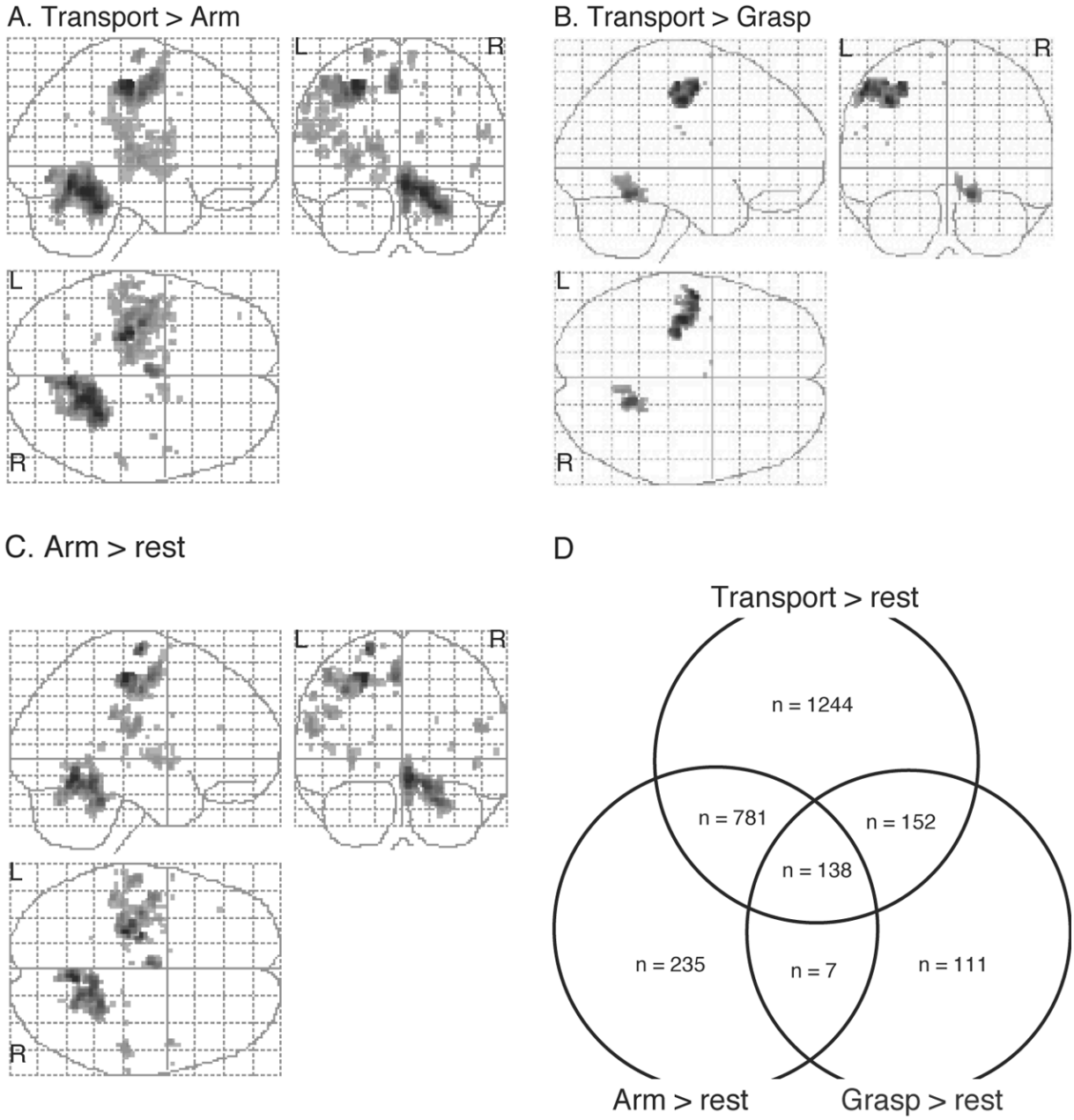

Fig. 4. Statistical parametrical maps (SPM*t*) illustrating activation loci of transport > rest (A), grasp > rest (B) and arm > rest (C). Topography of brain regions related to transport movements (A), grasp movements (B) and loaded arm movements (C) are expected to be revealed by these contrasts. (D) The numbers of voxels.

trasts (Fig. 4) and transport > arm and transport > grasp contrasts (Figs. 5 and 6), a conjunction analysis across subjects (Friston et al., 1999) was applied to find common activation to the subjects at the threshold of 5% corrected for multiple comparisons.

In the latter half of the analysis, the so-called factorial analysis was carried out to identify co-

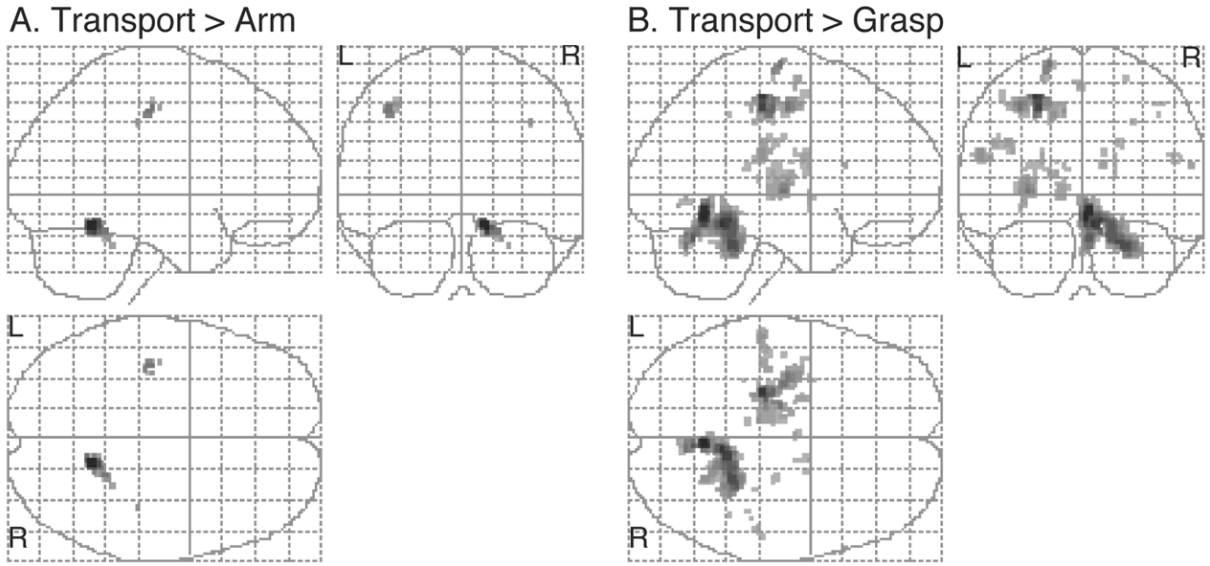

Fig. 5. Statistical parametrical maps (SPM*t*) illustrating activation loci of the transport > arm (A) and transport > grasp (B).

ordination-related brain regions (Fig. 8A). Namely, coordination-related areas were investigated in terms of the interaction between arm movement and grip force modulation effects: (a-b)–(c-d) (a, transport; b, loaded arm; c, grip force modulation; and d, rest). The resulting set of voxel values for each contrast constitutes a statistical parametric map of the *t* statistic, SPM*t*. Here, conjunction analysis was not utilized, and SPM99b was used.

Results

Fig. 4A–C shows the topography of brain regions related to object transport, grip force modulation and loaded arm movement, respectively. More specifically, they show statistical parametric maps (SPM*t*) illustrating the activation loci of transport > rest (A), grasp > rest (B), and arm > rest (C). The main effect of transport movement (Fig. 4A) was observed in many cerebral cortical areas including the bilateral sensory–motor cortices, bilateral premotor cortices, bilateral SMA, bilateral inferior frontal gyri, left middle frontal gyrus, bilateral cingulate gyri, bilateral inferior parietal lobules, right intraparietal sulcus, and bilateral insula (Table 1). The activity was also observed in the bilateral thalamus, basal ganglia, and cerebellum. In cerebral cortical areas, the thalamus and in the basal ganglia, activity was stronger in the contralateral (left) hemispheres to the using hand. This was not the case in the parietal cortex. However, the cerebellum had much stronger ipsilateral activation (Table 1). The main effect of grip force modulation (Fig. 4B) revealed activity in the left primary sensorimotor cortex, left premotor cortex, left SMA, left insula, and right anterior cerebellum, which are mainly small subsets of brain loci activated during transport movements. The primary effect of loaded arm movement (Fig. 4C) revealed activity in a wide range of regions including the left primary motor cortex, left premotor cortex, left SMA, bilateral postcentral gyri, inferior and middle frontal gyri, left cingulate gyrus, bilateral inferior parietal lobules, bilateral insula, bilateral thalamus, left basal ganglia, and the right anterior cerebellum, which are mainly large subsets of brain loci activated during transport movements.

Fig. 4D shows the numbers of activated voxels examined in the above three SPM contrasts in the format of the Venn diagram. One might first note that the number of activated voxels for transport movement was by far the largest, that for the loaded arm movement was medium, and that for the grasp was the smallest. A large portion (79%) of the arm-activated voxels was also activated in transport movement. Similarly, a large portion (71%) of the grasp-activated voxels was also activated in transport

Fig. 6. One slice with $z = -20$ mm in MNI coordinates showing a region of (transport > grasp) and (transport > arm) in the right anterior cerebellum. The open area shows the voxels that were more activated in transport than in grasp. The filled area shows the voxels that were more activated in transport than in arm. The mosaic area shows the conjunction of these two areas.

movement. On the other hand, a large portion (54%) of the transport-activated voxels was not activated in either arm or grasp movement.

Fig. 5 shows voxels that were more activated in transport than in loaded arm movement and those that were more activated in transport than in grasp movement, respectively. As expected from the results of Fig. 4, only the left primary motor cortex, right postcentral gyrus, and right anterior cerebellum were more activated in transport movements than in arm movements (Fig. 5A and Table 2). On the other hand, many brain loci, including the left primary motor cortex, left premotor cortex, left SMA, bilateral postcentral gyri, right inferior frontal gyrus, left cingulate gyrus, bilateral inferior parietal lobules, left thalamus, bilateral basal ganglia, and right anterior cerebellum, were more activated in transport than in grasp movements (Fig. 5B and Table 2).

TABLE 1

Principal areas of activation related to three movement tasks compared with the rest condition

	Transport > rest				Grasp > rest				Arm > rest			
	MNI coordinates			*t* value	MNI coordinates			*t* value	MNI coordinates			*t* value
L. BA4	−28	−22	54	10.24	−38	−18	44	5.00	−24	−26	52	9.03
R. BA4	38	−6	48	2.13								
L. BA6	−22	−16	72	4.06	−10	0	72	1.59	−22	−16	70	7.03
R. BA6	8	2	72	2.68								
L. SMA	−4	−8	56	6.00	−2	−4	54	1.64	−4	−10	52	5.17
R. SMA	10	−2	54	1.54								
L. postcentral gyrus	−54	−24	18	3.41	−58	−18	22	1.78	−58	−18	24	3.60
R. postcentral gyrus	58	−24	16	1.80					48	−26	22	3.21
L. inferior frontal gyrus	−52	−2	8	2.73					−60	4	28	2.04
R. inferior frontal gyrus									60	4	4	1.66
L. middle frontal gyrus	−40	48	0	1.96					−38	34	20	1.73
L. cingulate gyrus	−22	−10	42	1.64					−18	−10	40	1.68
R. cingulate gyrus	14	10	46	1.61								
L. inferior parietal lobule	−52	−34	48	2.40					−46	−34	28	3.59
R. inferior parietal lobule	52	−28	20	2.79					56	−26	26	1.60
R. intraparietal sulcus	26	−56	26	1.56								
L. insula	−40	2	16	3.25	−38	0	16	1.63	−44	−4	4	1.77
R. insula	46	4	−2	2.61					46	2	−4	2.72
L. thalamus	−18	−22	12	4.18					−18	−12	14	1.56
R. thalamus	14	−8	20	2.16					14	−28	0	1.57
L. basal ganglia	−28	−14	6	3.84					−32	−6	−2	3.06
R. basal ganglia	14	0	16	1.63								
R. cerebellum	14	−50	−16	10.35	16	−54	−18	3.76	6	−58	−12	7.85
L. cerebellum	−24	−42	−24	1.98								

$p < 0.05$, corrected. Activation peaks are reported in MNI coordinates. The MNI coordinates and *t* scores (degrees of freedom = 4481) for maxima of activations are presented. R and L indicate the right hemisphere and left hemisphere, respectively.

TABLE 2

Principal activations related to the transport task compared with two other movement tasks

	Transport > arm		Transport > grasp					
	MNI coordinates	*t* value	MNI coordinates	*t* value				
L. BA4	−40	−20	48	2.24	−26	−26	54	6.32
L. BA6					−18	−16	72	3.65
L. SMA					−2	−8	60	1.98
L. postcentral gyrus					−56	−26	20	2.59
R. postcentral gyrus	38	−28	40	1.86	50	−28	22	2.00
R. inferior frontal gyrus					60	20	16	1.91
L. cingulate gyrus					−16	−24	44	2.54
L. inferior parietal lobule					−40	−26	28	2.26
R. inferior parietal lobule					44	−32	50	1.76
L. thalamus					−22	−4	20	2.43
L. basal ganglia					−30	−14	2	3.59
R. basal ganglia					12	0	18	2.04
R. cerebellum	12	−54	−16	3.44	2	−58	−12	7.84

$p < 0.05$, corrected. Activation peaks are reported in MNI coordinates.

When we consider the conjunction of Fig. 5, then activated voxels were found only in the right anterior and superior cerebellum. That is, voxels that were simultaneously more activated in transport than in grasp movements, and more activated in transport than in arm movements were only found to exist in the cerebellum. Fig. 6 shows these activated voxels in the cerebellum at the slice of $z = -20$ mm of MNI coordinates. Here, the open areas show the voxels that were more activated in transport than in grasp. The filled areas show the voxels that were more activated in transport than in arm movement. The mosaic areas show the conjunction of these two areas and indicate the voxels that were simultaneously more activated in transport than in grasp and more activated in transport than in arm movement. The number of these conjointly activated voxels was 37.

The region of interest was defined as the above conjointly activated areas (mosaic, 37 voxels), and the relative blood oxygen level dependent (BOLD) signal increase compared with the rest condition was averaged over all voxels across all subjects. Fig. 7 shows that the BOLD signal increase was the largest for transport movements, slightly smaller for arm movements, and the smallest for grasp movements.

Finally, the coordination-related area was identified by the factorial analysis, which was explained in the latter half of the method. As shown in Fig. 8, the left biventer in the cerebellum was the only region identified as having a statistically significant relation to coordination (uncorrected $p < 10^{-4}$ for each voxel, larger than 62 voxels for cluster, corrected $p < 0.05$).

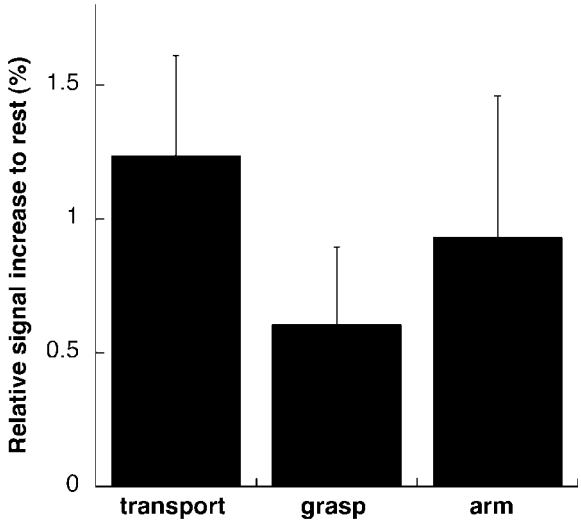

Fig. 7. Relative signal increase averaged across subjects in common regions of transport > grasp and transport > arm. Error bars show standard deviations between subjects.

Fig. 8B shows the relative BOLD signal in this region of interest (ROI). As shown in Fig. 8B, the mean BOLD signal in the ROI was higher under the rest condition (d) than under the other three conditions (a, b, and c); i.e. this region was deactivated by all movement tasks. The amount of deactivation by transporting task (a from d) was much smaller than the combined amount of deactivation by arm movement (b from d) and grip force modulation (c from d) tasks.

Discussion

Most regions related to arm movement and grip force modulation corresponded to those that were reported in many previous studies on simple hand or arm movement tasks (e.g. Fink et al., 1997). In particular, the coordinate of the peak *t*-score in grip force modulation (x, y, z in MNI coordinates: $-38, -18, 44$) in the primary sensorimotor cortex was located inferiorly and laterally to that found with arm movements ($-24, -26, 52$). This different location of peaks is congruent with the somatotopic organization of the hand and arm (Penfield and Rasmussen, 1950). Furthermore, in the anterior cerebellum the peak in grip force modulation ($16, -54, -18$) was located laterally to that found with arm movements ($6, -58, -12$). This difference in peak location is also congruent with previous findings that distal parts of the body are represented more laterally in the anterior cerebellum than more proximal parts of the body (Snider and Eldred, 1952; Grodd et al., 2001).

According to the computational model of grip force–load force coupling shown in Fig. 2C, the four different task conditions of Fig. 3 are expected to activate the three computational elements, the inverse model, the forward model and the grip force controller differently. None of the three elements is utilized in the rest condition. Only the grip force controller is activated for grip force modulation (grasp), and only the inverse model is activated for loaded arm movements (arm). On the other hand, all three

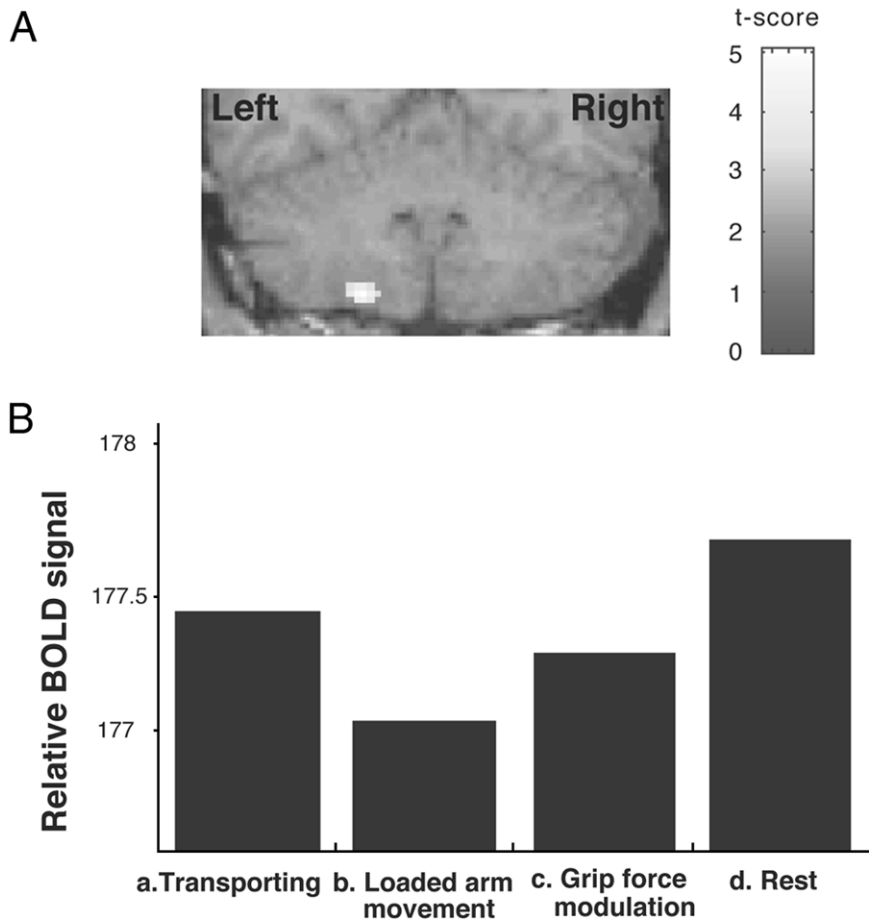

Fig. 8. Coordination-related activation superimposed on an anatomical coronal slice of a subject normalized to the MNI space. Only voxels with *t*-scores above 3.09 ($p < 10^{-4}$, uncorrected) were analyzed. We only found an active cluster of voxels in the left biventer of the cerebellum ($p < 0.05$, corrected on the basis of the random field theory). The MNI coordinates and *t*-score (df = 4481) for maxima of activations were −17, −58, −54 and 5.01. Adjusted BOLD contrast signals relative to the fitted mean in the cerebellar ROI related to coordination.

elements are utilized simultaneously for transport of the object. Consequently, with the transport > rest contrast shown in Fig. 4A, we expected to observe union of the activities of the three elements. For the grasp > rest contrast of Fig. 4B, activated voxels were assumed to contain activity of the grip force controller of Fig. 2C. Similarly, for the arm > rest contrast of Fig. 4C, we expected to observe activity related to the inverse model for arm. As Fig. 4D demonstrated, more than half of the activated voxels for the transport > rest contrast were not significantly more activated during either arm or grasp compared with the rest. Therefore, these voxels may contain activity of the forward model.

To further explore this possibility, the two contrasts transport > arm and transport > grasp were examined in Fig. 5. According to the computational model of Fig. 2C, the former contrast may reveal activity of the grip force controller and the forward model, while the latter may show activity of the inverse model and the forward model. Logically, the conjunction of the grip controller or the forward model and the inverse model or the forward model should reveal the locus of the forward model, and the conjunction of these is shown in Fig. 6. Only the small number of voxels in the right, anterior and superior cerebellum showed statistical significance, and may correspond to the forward model locus. The BOLD

signal increase for this ROI (Fig. 7) is compatible with the hypothesis that the ROI contains the forward model used for grip force–load force coupling.

If one simply assumes that the BOLD signal increases induced by activation in the three elements of Fig. 2C are linearly added to each other, the transport signal increase would have to be larger than the summation of the grasp increase and the arm increase because the forward model increase must also be added. However, this simple expectation was apparently not met, as shown by the BOLD signal of the right anterior cerebellum in Fig. 7. Consequently, in parallel to the above conjunction analysis, we further explored the possible forward model locus by the factorial analysis (a-b)–(c-d), based on this linear addition assumption (a = transport; b = loaded arm; c = grip force modulation; and d = rest). With the linear addition assumption, (a-b)–(c-d) should reveal only the forward model activation. Using these assumptions, multiple regression analysis showed that the left biventer in the cerebellum could be the only statistically significantly activated region involved in arm movement–grip force coordination. The previous conjunction analysis did not show this second ROI because it was deactivated by all movement tasks. This deactivation is consistent with the results of previous research that reported that hand movement could deactivate the cerebellum contralateral to the employed hand (Allison et al., 2000). The amount of deactivation by the transporting task was much smaller than the amount of summation of deactivation by the two simple movement tasks. Furthermore, the second ROI was more activated in the transporting task than in the arm movement or grip force modulation task. Therefore, according to the linear addition assumption, this ROI can be regarded as a potential coordination-related region.

The finding that the second ROI was in the left, i.e. contralateral, cerebellum strengthens the argument that this increased activation is related to coordination per se and not to grip force or arm movement control itself, since simple movements of a motor effector activate the anterior cerebellum ipsilaterally (Nitschke et al., 1996). Because most corticopontine projections and almost all cerebellar projections to the cerebral cortex are contralateral (Middleton and Strick, 1998), this activity in the left cerebellum during transport with the right hand is congruent with previous findings that lesions of the right cerebral cortex are often associated with ipsilateral impairments of complex sensorimotor tasks (Winstein and Pohl, 1995). More recently, Ehrsson et al. (2000) conducted an fMRI study with normal human subjects and found that the right cerebral cortex was engaged in a precision grip task performed with the right hand, although muscles of the left hand did not show reliable electromyogram (EMG) activity. Furthermore, Ehrsson et al. (2001) found that the right intraparietal cortex was more activated when subjects generate small grip forces than when they employ large grip forces. The small grip forces were representative of the forces that are typically used when manipulating small objects with precision grips in everyday situations. Thus, the left cerebellum together with the right cerebral cortex may be recruited in tasks more demanding than simple movement, in this case, coordination between the right arm and hand. Independently to the current work, Ehrsson et al. (2002) conducted a closely related fMRI experiment to examine cortical representations of coordinated grip and lift force control. Although their motivation was very similar to ours, the actual experimental paradigm was different. Their task was purely isometric and did not involve arm movement. The caudal two thirds of the cerebellum were not covered ($z > -22$ in the MNI standard space). They did not find any cerebellar activity in the coordination task compared with the other two tasks. They instead found that the coordination was specifically associated with activation of a posterior section of the right intraparietal cortex. The left biventar lobule activation, which we found, was outside their coverage, and might have anatomical connection with their right intraparietal cortex. Different experimental paradigms or different scanning coverage may explain the different results on right anterior cerebellum activity.

In summary, the same data were analyzed twice, in ways that are both expected to detect the additional activation due to coupled arm and grip action compared to either alone. The two analyses give different results, most spectacularly in that the cerebellar activation site shifts from right anterior cerebellum to left posterior. The different results obtained are due to different assumptions made in the two different analyses. In the first analysis, simple

overlap between arm and grasp conditions was assumed small, which was quantitatively supported by Fig. 4D. In the second analysis, linear summation assumption of BOLD signals corresponding to different brain functions was made, which should be wrong in general. However, as Fig. 8B shows, the left biventar activation was certainly larger during transport than arm or grip, thus the analysis was validated. Consequently, our data and the two analysis methods suggested that the right, anterior and superior cerebellum and/or biventer in the left cerebellum were the only regions related to grip force–load force coupling.

We hypothesized that the coordination-related regions include the neural substrate of the internal forward model. The present results suggest that the right anterior and superior cerebellum and/or the left biventer may contain such forward models. This supports the prediction by previous computational theories (Kawato et al., 1987; Kawato and Gomi, 1992; Miall et al., 1993; Wolpert et al., 1998; Kawato, 1999) that forward models are located in the cerebellum.

Finally, we compared the locations of the first and the second ROIs revealed in our study with the cerebellar locations of interests, which are related to forward models (Blakemore et al., 2001; Miall et al., 2001). The first ROI in the right, anterior and superior cerebellum is located approximately 25 mm medial and 20 mm superior to the right superior cerebellar locus, which was found to be significantly correlated with the delay in the self-tickling task of Blakemore et al. (2001). Both studies involved right arm and hand movement, but ours involved grip force modulation while theirs involved perceptual modulation due to forward model prediction. Since cancellation of tactile sensation due to self-movement is thought to be more cognitive than grip force–load force coupling as motor coordination, the more lateral and inferior location of more cognitive forward models is not surprising. The second ROI, in the left biventar location in our study is about 15 mm medial and 20 mm inferior to the locus that was found to be correlated with asynchrony and independence of eye–hand coordination by Miall et al. (2001). Both studies involved right hand movements, but ours dealt with arm–hand coordination while theirs dealt with eye–hand coordination. Physically, the arm and hand are coupled more closely, and the grip force–load force coupling tasks may be interpreted as a more basic form of motor coordination. Thus, it was not surprising to find the more sophisticated eye–hand coordination induced more lateral and more superior activation near the bottom of the left cerebellum.

In the current behavioral paradigm, the forward model predicts future arm movement and load force from the efference copy of the arm motor command. Recent studies have rigorously demonstrated that the cerebellum plays an essential role in the coordination of movements with multiple degrees of freedom (Bastian et al., 1996). In this study, we supported a specific computational model of coordination as shown in Fig. 2C. That is, we explained the coupling of grip force and load force by the mechanism where the forward model in the cerebellum predicts a trajectory of one motor effector (arm) and this prediction is used to control another motor effector (hand). Apparently, this computational framework can be generalized to arbitrary pairs of motor effectors such as eye and hand (Scarchilli and Vercher, 1999; Miall et al., 2000, 2001) and right and left hands; moreover, the framework might be considered a general principle of coordination.

Conclusions

The present experiment adopted a factorial deconvolution of the transporting task when subjects transported an object with a precision grip using the right arm and hand. The obtained imaging data suggested that the right, anterior and superior cerebellum and/or biventer in the left cerebellum were the only regions related to grip force–load force coupling. This agrees with previous findings that the right cerebral cortex is involved in more complex precision grip tasks than simple motor control while using the right hand. Furthermore, from a computational viewpoint, these cerebellar regions might contain forward models of arm movements.

References

Allison, J.D., Meador, K.J., Loring, D.W., Figueroa, R.E. and Wright, J.C. (2000) Functional MRI cerebral activation and deactivation during finger movement. *Neurology*, 54: 135–142.

Bastian, A.J., Martin, T.A., Keating, J.G. and Thach, W.T. (1996) Cerebellar ataxia: abnormal control of interaction torques across multiple joints. *J. Neurophysiol.*, 76: 492–509.

Blakemore, S.J., Wolpert, D.M. and Frith, C.D. (1998) Central cancellation of self-produced tickle sensation. *Nat. Neurosci.*, 1: 635–640.

Blakemore, S.J., Wolpert, D.M. and Frith, C.D. (1999) The cerebellum contributes to somatosensory cortical activity during self-produced tactile stimulation. *Neuroimage*, 10: 448–459.

Blakemore, S.J., Frith, C.D. and Wolpert, D.M. (2001) The cerebellum is involved in predicting the sensory consequences of action. *Neuroreport*, 12: 1879–1884.

Ehrsson, H.H., Fagergren, A., Jonsson, T., Westling, G., Johansson, R.S. and Forssberg, H. (2000) Cortical activity in precision versus power-grip tasks: an fMRI study. *J. Neurophysiol.*, 83: 528–536.

Ehrsson, H.H., Fagergren, A. and Forssberg, H. (2001) Differential fronto-parietal activation depending on force used in a precision grip task: an fMRI study. *J. Neurophysiol.*, 85: 2613–2623.

Ehrsson, H.H., Fagergren, A., Jonsson, T., Johansson, R.S. and Forssberg, H. (2002) Cortical representation of fingertip forces used in human manipulation: grip force, lift force and coordinated grip and lift forces. *J. Neurophysiol*., submitted.

Fink, G.R., Frackowiak, R.S.J., Pietrzyk, U. and Passingham, R.E. (1997) Multiple nonprimary motor areas in the human cortex. *J. Neurophysiol.*, 77: 2164–2174.

Flanagan, J.R. and Tresilian, J.R. (1994) Grip–load force coupling: a general control strategy for transporting objects. *Exp. Psychol. Hum. Percept. Perform.*, 20: 944–957.

Flanagan, J.R. and Wing, A.M. (1995) The stability of precision grip force during cyclic arm movements with a hand-held load. *Exp. Brain Res.*, 105: 455–464.

Flanagan, J.R. and Wing, A.M. (1996) Internal models of dynamics in motor learning and control. *Soc. Neurosci. Abstr.*, 22(2): 897.

Flanagan, J.R. and Wing, A.M. (1997) The role of internal models in motion planning and control: evidence from grip force adjustments during movements of hand-held loads. *J. Neurosci.*, 17: 1519–1528.

Friston, K.J., Holmes, A.P., Worsley, K.J., Poline, J.P., Frith, C.D. and Frackowiak, R.S.J. (1995) Statistical parametric maps in functional imaging: A general linear approach. *Hum. Brain Mapp.*, 2: 189–210.

Friston, K.J., Holmes, A.P., Price, C.J., Buchel, C. and Worsley, K.J. (1999) Multisubject fMRI studies and conjunction analyses. *NeuroImage*, 10: 385–396.

Gomi, H. and Kawato, M. (1996) Equilibrium-point control hypothesis examined by measured arm-stiffness during multi--joint movement. *Science*, 272: 117–120.

Gomi, H., Shidara, M., Takemura, A., Inoue, Y., Kawano, K. and Kawato, M. (1998) Temporal firing patterns of Purkinje cells in the cerebellar ventral paraflocculus during ocular following responses in monkeys I. Simple spikes. *J. Neurophysiol.*, 80: 818–831.

Grodd, W., Hulsmann, E., Lotze, M., Wildgruber, D. and Erb, M. (2001) Sensorimotor mapping of the human cerebellum: fMRI evidence of somatotopic organization. *Hum. Brain Mapp.*, 13: 55–73.

Imamizu, H., Miyauchi, S., Tamada, T., Sasaki, Y., Takino, R., Putz, B., Yoshioka, T. and Kawato, M. (2000) Human cerebellar activity reflecting an acquired internal model of a new tool. *Nature*, 403: 192–195.

Johansson, R.S. (1996) Sensory control of dexterous manipulation in humans. In: A.M. Wing, P. Haggard and J.R. Flanagan (Eds.), *Hand and Brain: The Neurophysiology and Psychology of Hand Movements*. Academic, New York, pp. 381–414.

Johansson, R.S. and Westling, G. (1984) Roles of glabrous skin receptors and sensorimotor memory in automatic control of precision grip when lifting rougher or more slippery objects. *Exp. Brain Res.*, 56: 550–564.

Jordan, M.I. and Rumelhert, D.E. (1992) Forward models: Supervised learning with a distal teacher. *Cogn. Sci.*, 16: 307–354.

Kawato, M. (1999) Internal models for motor control and trajectory planning. *Curr. Opin. Neurobiol.*, 9: 718–727.

Kawato, M. and Gomi, H. (1992) The cerebellum and VOR/OKR learning models. *Trends Neurosci.*, 15: 445–453.

Kawato, M., Furukawa, K. and Suzuki, R. (1987) A hierarchical neural-network model for control and learning of voluntary movement. *Biol. Cybern.*, 57: 169–185.

Kitazawa, S., Kimura, T. and Yin, P.B. (1998) Cerebellar complex spikes encode both destinations and errors in arm movements. *Nature*, 392: 494–497.

Kobayashi, Y., Kawano, K., Takemura, A., Inoue, Y., Kitama, T., Gomi, H. and Kawato, M. (1998) Temporal firing patterns of Purkinje cells in the cerebellar ventral paraflocculus during ocular following responses in monkeys. II. Complex spikes. *J. Neurophysiol.*, 80: 832–848.

Mehta, B. and Schaal, S. (2002) Forward models in visuomotor control. *J. Neurophysiol.*, in press.

Miall, R.C., Weir, D.J., Wolpert, D.M. and Stein, J.F. (1993) Is the cerebellum a Smith predictor? *J. Mot. Behav.*, 25: 203–216.

Miall, R.C., Imamizu, H. and Miyauchi, S. (2000) Activation of the cerebellum in co-ordinated eye and hand tracking movements: an fMRI study. *Exp Brain Res.*, 135: 22–33.

Miall, R.C., Reckess, G.Z. and Imamizu, H. (2001) The cerebellum coordinates eye and hand tracking movements. *Nat. Neurosci.*, 4: 638–644.

Middleton, F.A. and Strick, P.L. (1998) The cerebellum: an overview. *Trends Cogn. Sci.*, 2: 348–354.

Nitschke, M.F., Kleinschmidt, A., Wessel, K. and Frahm, J. (1996) Somatotopic motor representation in the human anterior cerebellum. A high-resolution functional MRI study. *Brain*, 119: 1023–1029.

Penfield, W. and Rasmussen, T. (1950) *The Cerebral Cortex of Man: A Clinical Study of Localization of Function*. Macmillan, New York.

Scarchilli, K. and Vercher, J.L. (1999) The oculomanual coordination control center takes into account the mechanical properties of the arm. *Exp. Brain Res.*, 124: 42–52.

Shidara, M., Kawano, K., Gomi, H. and Kawato, M. (1993)

Inverse-dynamics model eye movement control by Purkinje cells in the cerebellum. *Nature*, 365: 50–52.

Snider, R.S. and Eldred, E. (1952) Cerebro-cerebellar relationships in the monkey. *J. Neurophysiol.*, 15: 27–40.

Takemura, A., Inoue, Y., Gomi, H., Kawato, M. and Kawano, K. (2001) Change in neuronal firing patterns in the process of motor command generation for the ocular following response. *J. Neurophysiol.*, 86: 1750–1763.

Vercher, J.-L., Sarès, F., Blouin, J., Bourdin, C. and Gauthier, G. (2003) Role of sensory information in updating internal models of the effector during arm tracking. In: C. Prablanc, D. Pélisson and Y. Rossetti (Eds.), *Neural Control of Space Coding and Action Production. Progress in Brain Research*, Vol. 142. Elsevier, Amsterdam, pp. 203–222 (this volume).

Vetter, P., Wolpert, D.M. and Flanagan, J.R. (2002) Prediction precedes control in motor learning. (submitted for publication).

Winstein, C.J. and Pohl, P.S. (1995) Effects of unilateral brain damage on the control of goal-directed hand movements. *Exp. Brain Res.*, 105: 163–174.

Wolpert, D.M. and Kawato, M. (1998) Multiple paired forward and inverse models for motor control. *Neural Networks*, 11: 1317–1329.

Wolpert, D.M., Ghahramani, Z. and Jordan, M.I. (1995) An internal model for sensorimotor integration. *Science*, 269: 1880–1882.

Wolpert, D.M., Miall, C. and Kawato, M. (1998) Internal models in the cerebellum. *Trends Cogn. Sci.*, 2: 338–347.

Yamamoto, K., Kobayashi, Y., Takemura, A., Kawano, K. and Kawato, M. (2002) Computational studies on the acquisition and adaptation of ocular following responses based on the synaptic plasticity in the cerebellar cortex. *J. Neurophysiol.*, 87: 1554–1571.

?#2

QUERIES:

?#1: Please check the word ‘sinc’. (page 178)
?#2: Submitted to which journal? (page 188)